EPR Dosimetry Of Synthesized Nano-Crystalline Hydroxyapatite: Effect Of Making Procedure

Nahid Hajiloo (nhajiloo@aeoi.org.ir)
Nuclear Science and Technology Research Institute
Farhood Ziaie
Nuclear Science and Technology Research Institute

Research Article

Keywords:

Posted Date: February 22nd, 2022

DOI: https://doi.org/10.21203/rs.3.rs-1354857/v1

Abstract

The EPR response of hydroxyapatite (HAP) samples was studied from a dosimetric standpoint in this paper. The HAP samples were prepared from several ways for this aim. Under the ^{60}Co-source radiation, the synthesized samples were irradiated at various absorbed doses ranging from 0.1 to 45 kGy. HAP samples' EPR response in air was tested at room temperature. The peak-to-peak signal amplitude was then obtained from the difference in EPR signal intensities. The findings show the role of making procedure and subsequently particle size, carbon impurity and morphology in EPR response.

1. Introduction

Hydroxyapatite, is considered as critical substances contained in bone and enamel for Electron Paramagnetic Resonance (EPR) retrospective dosimetry and archaeological dating (Rink, 1997; Grün et al., 1991; Huang et al., 1993). Doses are measured in the mineral component of calcified tissues by detecting concentrations of paramagnetic species caused by radiation. Using EPR spectra of irradiated biological and synthetic apatite, several paramagnetic entities, including, , , , and of varied symmetries, have been found (Doi et al., 1997; Moens et al., 1991). CO_3^{3-} groups by occupying PO_4^{2-} or OH^- sites in the hydroxyapatite (HAP) structure, produce almost all of them. Some authors have been already noticed that the EPR spectra of carbonated apatite depends on conditions under which the samples were prepared (Callens et al. 1991; Oliveira et al. 2000).

In this research synthesized HAP samples were made through some different procedures. Therefore, they have various carbon impurity, morphology, grain size, and crystallinity, because of the different preparation conditions and initial raw materials. Following pre-treatment, the samples were irradiated at various gamma high doses before being measured for EPR. From a dosimetric standpoint, the signal intensity variations were compared to each other and the bone sample.

2. Procedure For The Experiment

2.1. HAP making procedures

The required HAP samples were synthesised using eight distinct processes that have previously been published by various scientists. This section explains these methods in detail. Also, the standard identical hydroxyapatite (MK), achieved from Merck Company was utilized to ensure that the final product was hydroxyapatite. Merck Company also provided all of the raw materials needed in this project.

2.1.1. Planetary Mill

This sample was prepared by grinding MK as a starting material for 12 hours in acetone in a Fritsch 6 series planetary ball mill machine. The final sample was named AS.

2.1.2 Sol-Gel (1)

A 0.5 mol/l solution was achieved by dissolving Phosphoric pent oxide (P2O5) in 100% ethanol. In addition, a predetermined amount of (Ca $(NO_3)_2.4H_2O$) was dissolved in 100% ethanol to generate a 1.67mol/l solution. The Ca/P molar ratio was 1.67 for the initial mixed precursor solution. Continuous mixing at room temperature for 24 hours resulted in the formation of a white transparent gel. For 24 hours at 80°C, the gel was dried in an electric air oven. Individually heated at 600°C at a rate of 5°C/min in a muffle furnace, the dried gel was then placed in air to cool to ambient temperature (Fathi et al., 2007). The obtained sample was designated as SG1.

2.1.3. Sol-Gel (2)

At a steady temperature of 85°C and vigorous stirring, 0.5M of (Ca $(NO_3)_2.4H_2O$) in ethanol with a pH of 10.5 was added to 0.5M of $(NH_4)2PO_4$ with the rate of 5ml/min. For 4 hours, the resulting sol–gel was constantly stirred at pH = 10 (pH was maintained constant by adding Ca $(OH)_2$ solution) at 85°C, which was constant. After cooling, the product was kept at 40°C overnight in the oven. Then for two hours, the product was sintering at 600°C (Anee Kuriakose et al., 2004). The obtained sample was designated as SG_2.

2.1.4. Fluid body simulation (FBS)

Nano-crystalline apatite was made using a biomimetic technique. In order to make TTCP, a 1:1 molar ratio of calcium carbonate and declaim phosphate anhydrous was heated at 1500°C for 6 hours, after that quickly cooled to room temperature. Then the final TTCP product milled for six hours. Phosphate solution (DHP) was mixed with 3g/ml acidic calcium phosphate, brushite, and an alkali-basic tetra-calcium chloride (TTCP) to form a settable calcium phosphate paste. The paste has to be maintained in fluid body simulated solution (FBS), which has an ionic composition similar to human plasma, for seven days. At the end of the immersion period, the material was taken from the FBS, rinsed with distilled water, dried at 70°C, and ground into a fine powder using a planetary mill (Hesaraki et al., 2009). The acquired sample was referred to as FBS.

2.1.5. Hydrolysis

$CaHPO_4.2H_2$, DCPD (calcium hydrogen phosphate dihydrate) and $CaCO_3$ were combined with Ca/P ratios (1.67) (HAP ratio). The admixture was then added into 500 ml of 2.5 M (pH = 13) and stirred for 1 hour in 75°C high-speed agitator. The reaction was stopped after hydrolysis through cooling in icy water. Deionized water was used to wash the aggregates five times. Drying at 60°C and grinding were performed on the synthetic materials before they could be put to use. Hy_2 is the name given to this substance. The powder was annealed in air at 600°C for 4 hours at a heating rate of 1C/min (Jen Shih et al., 2004). The final material was coded as Hy_1.

2.1.6. Microwave

A well-ground mixture of $CaCl_2$ and Na_3PO_4 with a molar ratio of 1.67:1 was reacted in a home-made microwave oven (800W) for 30 min to produce hydroxyapatite powder. The particles were washed with

water to eliminate sodium chloride, as a by-product of the process, and dried at 80°C (Parhi et al., 2006). Mic was the name given to the collected sample.

2.2. Characterization

X-ray diffraction (XRD) analysis was carried out using a Philips Analytical X-Ray B.V and Ni-filtered CuK radiation in the 2 θ range of 20°- 60°. As illustrated in Eq. 1, Scherer's equation was used to determine the grain size of powders that had been manufactured.

$$t = \frac{0.89\lambda}{B\cos\theta} \qquad (1)$$

Where t is the size of grain, λ is X-ray tube wavelength, B is the width at half maximum of peak of X-ray, and θ is the angle Bragg.

The HAP particle size was investigated using a Phillips Company XL-30 series scanning electron microscope (SEM). Using the LaB6 filament, the system's magnification can range from 25x to 400000x. Prior to the SEM examinations, a thin layer of gold was applied to the sample surfaces.

Transmission electron microscopy (TEM) instruments from the EM208S series were used to examine the particles' size and shape.

Fourier transmission infrared spectroscopy (FTIR) spectra were taken on samples in the wave number range using an ATI Mattson Genesis series, made in the United States. An Eltra CS-2000 Carbon/Sulfur instrument was used for carbon analysing of the materials.

2.3. Sample irradiation

The samples were weighted and packaged in a plastic cover to irradiate with a Russian-made ^{60}Co-ray source facility (PX-30 series) with a dose rate of 15.6 Gy/min. The samples were irradiated with gamma doses ranging from 0.1 to 45 kGy.

2.4. EPR measurement

The samples were placed in quartz thin-wall EPR tubes (4 mm diameter) and analyzed in the X-band with a Bruker EMS-104 spectrometer. Peak to peak height (First Derivative Absorption Spectrum) per sample mass was used to compute EPR Signal Intensities. The samples were analyzed at the same instrument settings to guarantee the reproducibility of EPR signal strength. The standard deviation of each sample's mean EPR measurement was estimated, and it was found to be less than 3% for all readings. There were four scans performed with an EPR spectrometer set to the following parameters: 0.285-mT modulation amplitude, 100-kHz modulation frequency, 3.0-mT scan width, 1024-point field resolution, 164-msec time constant, 21-sec sweep duration, 50-dB receiver gain, and a total of four scans.

3. Results And Discussion

The XRD patterns of the standard HAP and generated SG1 samples are shown in Figs. 1a and 1b. In compared to the standard sample, all identified peaks on this sample are associated to the hydroxyapatite phase (JCPDS Card, 1994). The lines seen at 865cm-1 and 1400–1500 cm^{-1} in the FTIR spectrum of the SG1 sample (Fig. 2) are attributed to $^{2-}CO_3$ (low C–O area) and $^{3-}CO_3$ (high C–O region), respectively, indicating carbonate substitution for PO4 in the apatite lattice (Kweh et al., 2002). HPO4 is the band that can be seen around 890 cm (Ishikawa et al., 1999). The XRD pattern and FTIR spectra of the other samples are also very comparable to this one. Calculations according to the Eq. 1 and using the sample XRD patterns were made to obtain the particle size. These results along with the percentage of carbon impurity of the samples are depicted in Table 1.

The structural features of the HAP crystals are visible in SEM images of the samples (Fig. 3). Figure 4 shows the TEM images of the HAP powders prepared via different methods, as well. The crystallinity and morphology of each sample can be seen from these images. The particle size predicted using Scherer's equation is confirmed by SEM and TEM images. The EPR signal strength as a function of absorbed dose for all samples is shown in Fig. 5 for a dose range of 0.1 kGy to 45 kGy.

The particle size and amount of carbon impurity have a crucial impact in EPR dosimetry employing the HA powder, as shown in Table 1 and Fig. 5. According to the Fig. 5 the SG1 with about 30 nm particle size and 0.47% carbon impurity, has the highest EPR response. As a matter of fact, comparing the pairs of SG1, SG2 and MK, As, having the same carbon impurities but a different grain size, as could be predicted, it concluded from Fig. 5 that the sample with larger grain size have a lower EPR response. On the other hand, the samples Mic and SG1 with almost the same grain size and a different carbon impurities (Mic is lower) confirm the aforementioned word about the importance of carbon content in HA samples.

In addition Hy1 and Hy2 synthesized from the same method but they have some different characteristics such as particle size, carbon impurity and crystallinity, then Hy2 with ~ 10 nm particle size and 1.03% carbon impurity has EPR response several times higher than Hy1 with ~ 46 nm particle size and 0.72% carbon.

As mentioned, the samples of Hy1 and Hy2 are both synthesized by the same method and the only difference is in the annealing process, which causes the two samples to have different crystallinity, shape, crystal dimensions and carbon impurity. As can be seen in the SEM images of these two samples (Figs. <link rid="fig3">3</link>-d and 3-h), Hy2 does not have a specific crystalline shape and its crystallinity is very low, while Hy1 has a high crystallinity and its crystalline shape is spherical.

By comparing SG1 (~ 30 nm, 0.47%) and Hy2 (~ 10, 1.03%), from Fig. 5 SG1 has higher EPR response than Hy2 with smaller particle size and higher carbon impurity, this phenomenon shows the morphology and crystallinity effect.

As a result, the size of the crystals, the quantity of carbon in them, as well as their form and crystallinity percentage, all have a role in the EPR response of HAp samples. The dimensions of the samples and the amount of carbon will be essential when the crystallinity and crystal shape of the samples are not

considerably different from one another. As the dimensions of the crystals decrease and their carbon content increases, the signal intensity increases.

Overall, samples with smaller particle size and higher carbon impurity have better response. Optimum carbon impurity and morphology effect could be discussed separately.

Table 1
Particle size and carbon content of synthesized HAP samples.

Sample Code	SG1	Mk	BFS	AS	SG2	Hy1	Hy2	Mic
particle Size from Scherer's equation	32	-	22	29	27.8	46	10	95
particle Size from TEM	25–30	100–300	25–50	20–300	50–175	46	10	150–700
Carbon Impurity (%)	0.47	0.3	0.34	0.3	0.47	0.72	1.03	0.26

4. Conclusions

The synthesis parameters play a major effect in dosimetry with hydroxyapatite powder, according to this study.

The maximum dose response was achieved with the "SG1" sample with a grain size of ~30 nm and a carbon impurity of 0.47 percent. Samples with similar grain sizes and lower carbon percent that were synthesized using the same procedure had far lower EPR signal strength. Among samples with the same carbon percentage and different average grain size (MK and AS), sample with lower grain size has higher EPR signal intensity.

These results reinforce previous investigations which indicate carbon importance in dosimetry with HAp and have been illustrate grain size role.

In addition, it is considerable that among a sample with ~30 nm particle size and 0.47% carbon impurity (SG1) and another with ~10 particle size and 1.03% carbon impurity (Hy2), the first one has higher EPR response that confirm morphology effect of sample.

Declarations

Contributions

F. Z developed the idea and N.H did the measurements and manuscript writing.

References

1. Callens, F.J., Verbeeck, R.M.H., Moens, P.D. 1991. An EPR study of intact and powdered human tooth enamel dried at 400°C. Calcif. Tissue Int. 56, 543–548.
2. Doi, Y., Aoba, T., Okazaki, M., Takahashi, J., Moriwaki, Y. 1979. Analysis of paramagnetic centers in X-ray-irradiated enamel, bone and carbonate-containing hydroxyapatite by electron spin resonance spectroscopy. Calcif. Tissue Int. 28, 107–112.
3. Fathi, M.H., Hanifi, A. 2007. Evaluation and characterization of nanostructure hydroxyapatite powder prepared by simple sol–gel method. Materials Letters 61, 3978–3983.
4. Grun, R., 1993. Status and present problems in ESR dating. Appl. Radiat. Isot. 40, 1045–1055.
5. Hesaraki, S., Moztarzadeh, F., Nemati, R., Nezafati, N., 2009. Preparation and characterization of calcium sulfate-biomimetic apatite nanocomposites for controlled release of antibiotics. J. Biomed. Mater. Res. B (Appl Biomater), 2009 Nov; 91(2):651 – 61.
6. Huang, P., Jin, S., Peng, Z., Liang, R., Lu, Z., Wan, Z., Chen, J., Yuan, Z. 1993. ESR dating of tooth enamel: comparison with U-series, FT and TL dating at the Peking man site. Appl. Radiat. Isot. 44, 239.
7. Ishikawa, K., Takagi S., Chow, L.C., Suzuki, K. 1999. Reaction of calcium phosphate cements with different amounts of tetracalcium phosphate and dicalcium phosphate anhydrous. J Biomed Mater Res A; 46:405–510. JCPDS Card.1994, 9–432.
8. Jen, S.W., Feng, C.Y., Chin, W.M., Hsiung, H.M. 2004. Crystal growth and morphology of the nano-sized hydroxyapatite powders synthesized from $CaHPO_4$,$2H_2O$ and $CaCO_3$ by hydrolysis method. Journal of Crystal Growth. 270, 211–218.
9. Kuriakose, T. A., Kalkura, S. N., Palanichamyc, M., Arivuolid, D., Dierkse, K., Bocellif, G., Betzel, C. 2004. Synthesis of stoichiometric nano crystalline hydroxyapatite by ethanol-basedsol–gel technique at low temperature. Journal of Crystal Growth 263, 517–523.
10. Kweh, S.W.K., Khor, K.A., Cheang, P. 2002. An in vitro investigation of plasma sprayed hydroxyapatite (HA) coatings produced with flame-spheroidized feedstock. Biomaterials. 23,775–785.
11. Moens, P.D., Callens, F., Matthys, P., Maes, F. 1991. Adsorption of carbonate-derived molecules on the surface of carbonate-containing apatite. J. Chem. Soc. Faraday Trans. 87: 19, 3137–3141.
12. Oliveira, L.M., Rossi, A.M., Lopes, R.T., 2000. Gamma dose response of synthetic A-type carbonated apatite in comparison with the response of tooth enamel. Appl. Radiat. And Isot. 52, 1093–1097
13. Parhi, P., Ramanan, A., Alok, R., Ray, R. 2006. Synthesis of nano-sized alkaline-earth hydroxyapatites through microwave assisted metathesis route. Materials Letters 60, 218–221.
14. Rink, W.J. 1997. Electron Spin Resonance (ESR) dating and ESR applications in Quaternary Science and Archaeometry. Rad. Meas. 27, 975–1025.

Figures

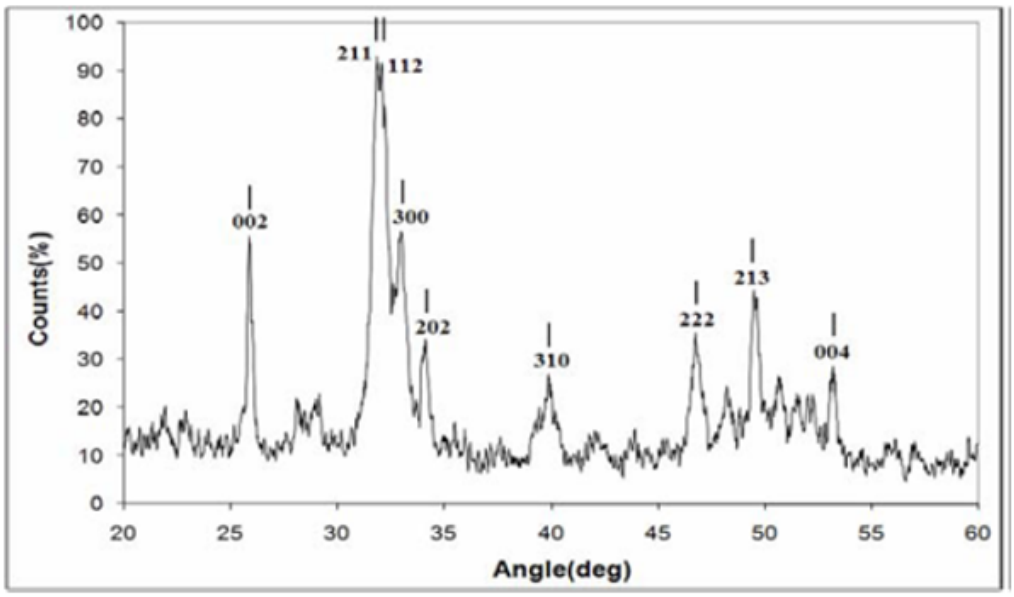

(a)

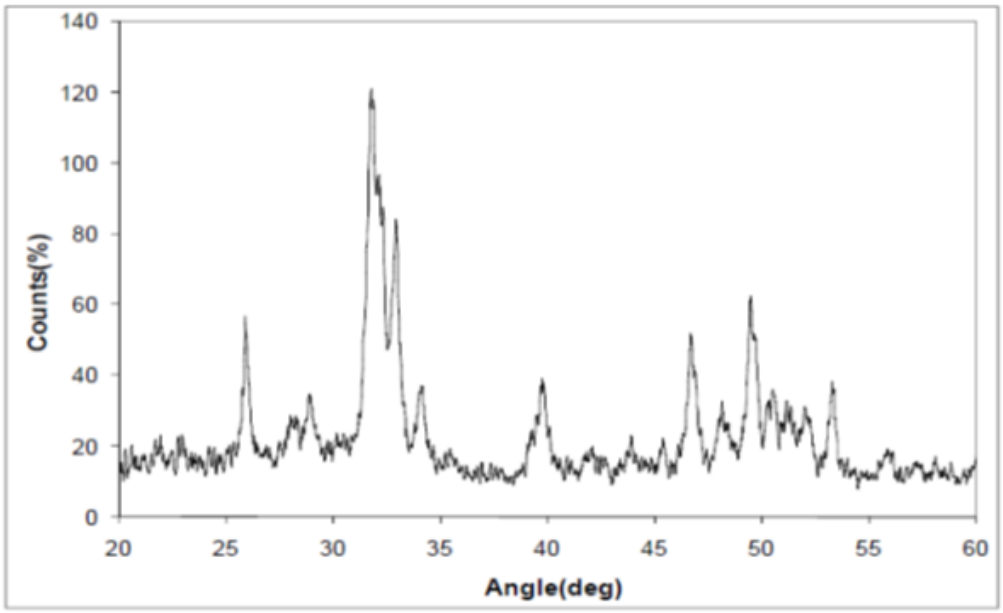

(b)

Figure 1

XRD pattern of the a) standard sample (Merck) and b) synthesized SG1 sample.

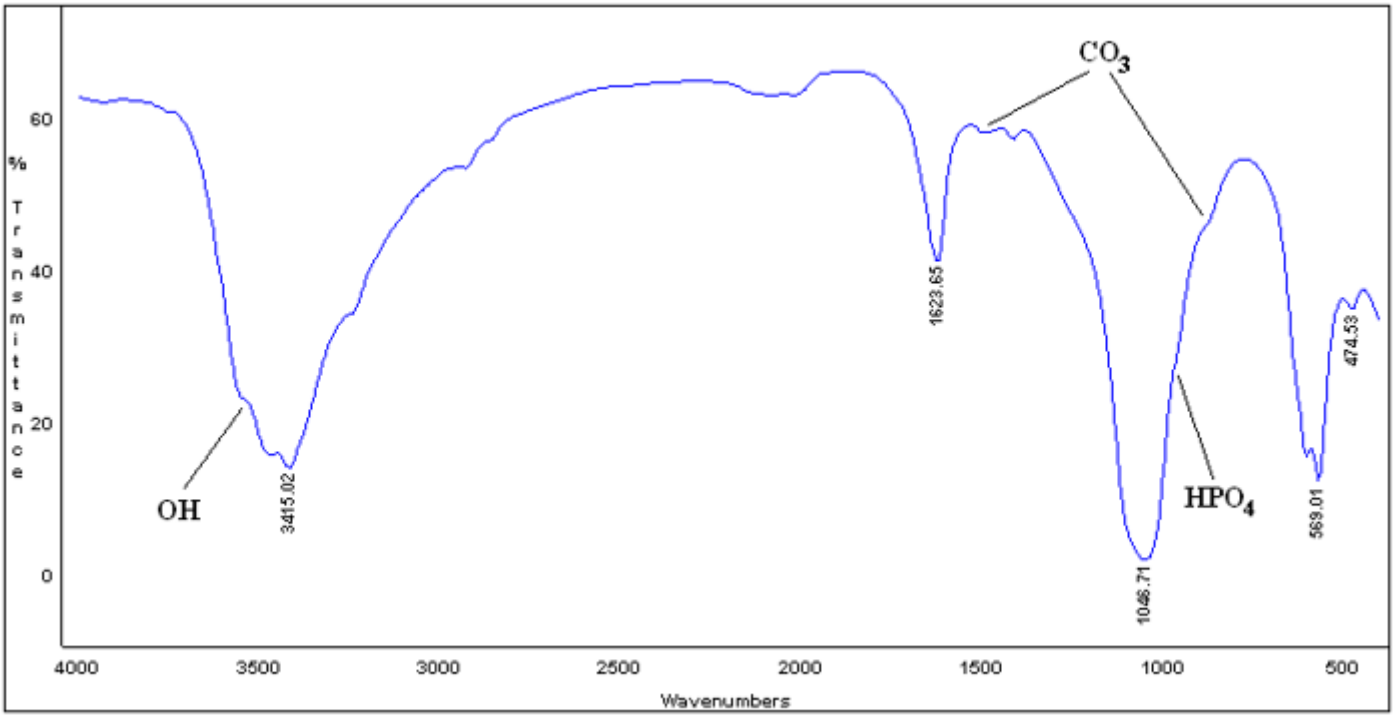

Figure 2

FTIR pattern of the SG1 sample.

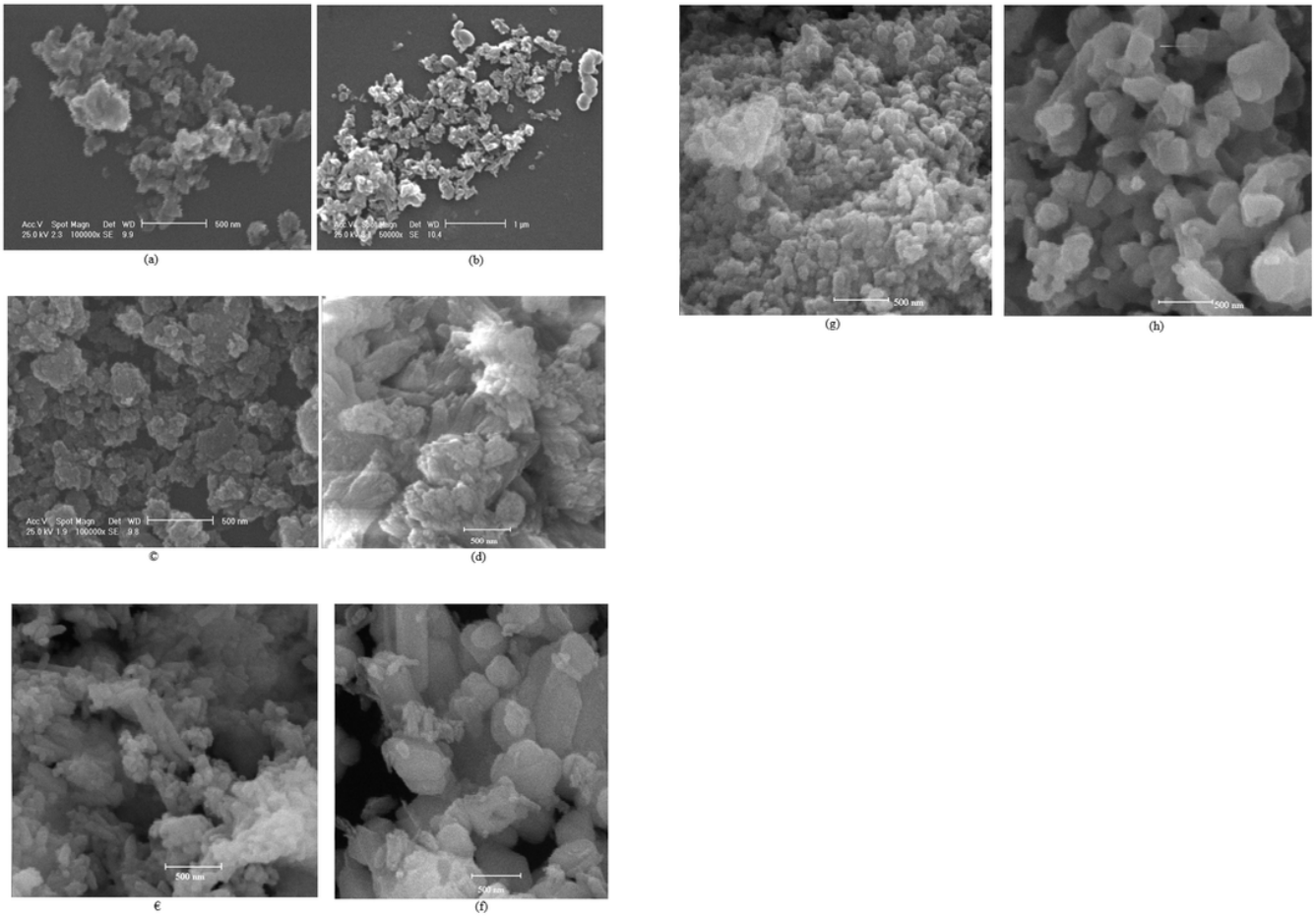

Figure 3

SEM micrograph of, a) SG1; b) MK; c) FBS; d) Hy2; e) SG2; f) Mic; g) AS and h) Hy1 samples.

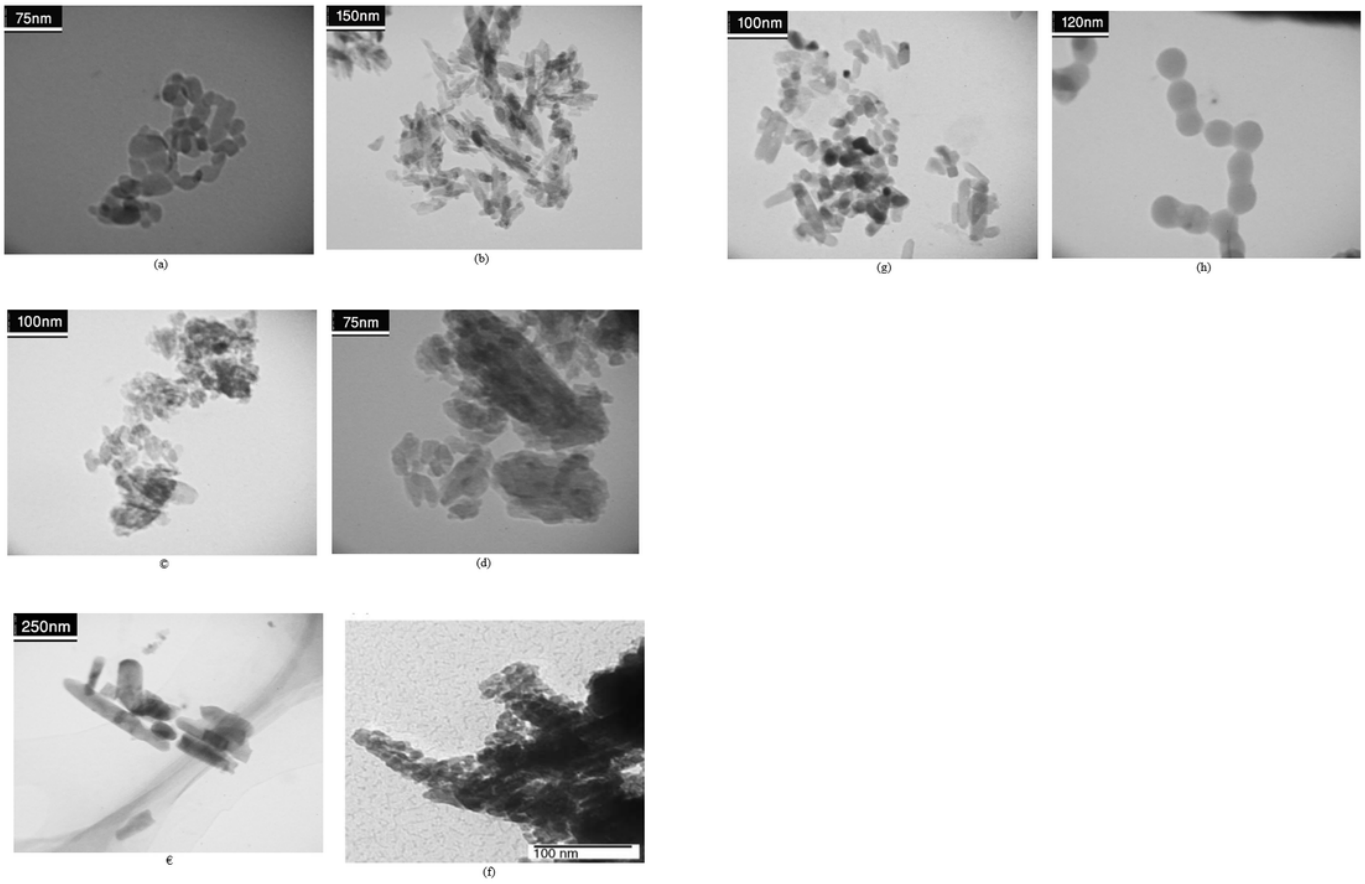

Figure 4

TEM micrograph of, a) SG,1; b) MK; c) FBS; d) Hy2; e) SG2; f) Mic; g) AS and h) Hy1 samples.

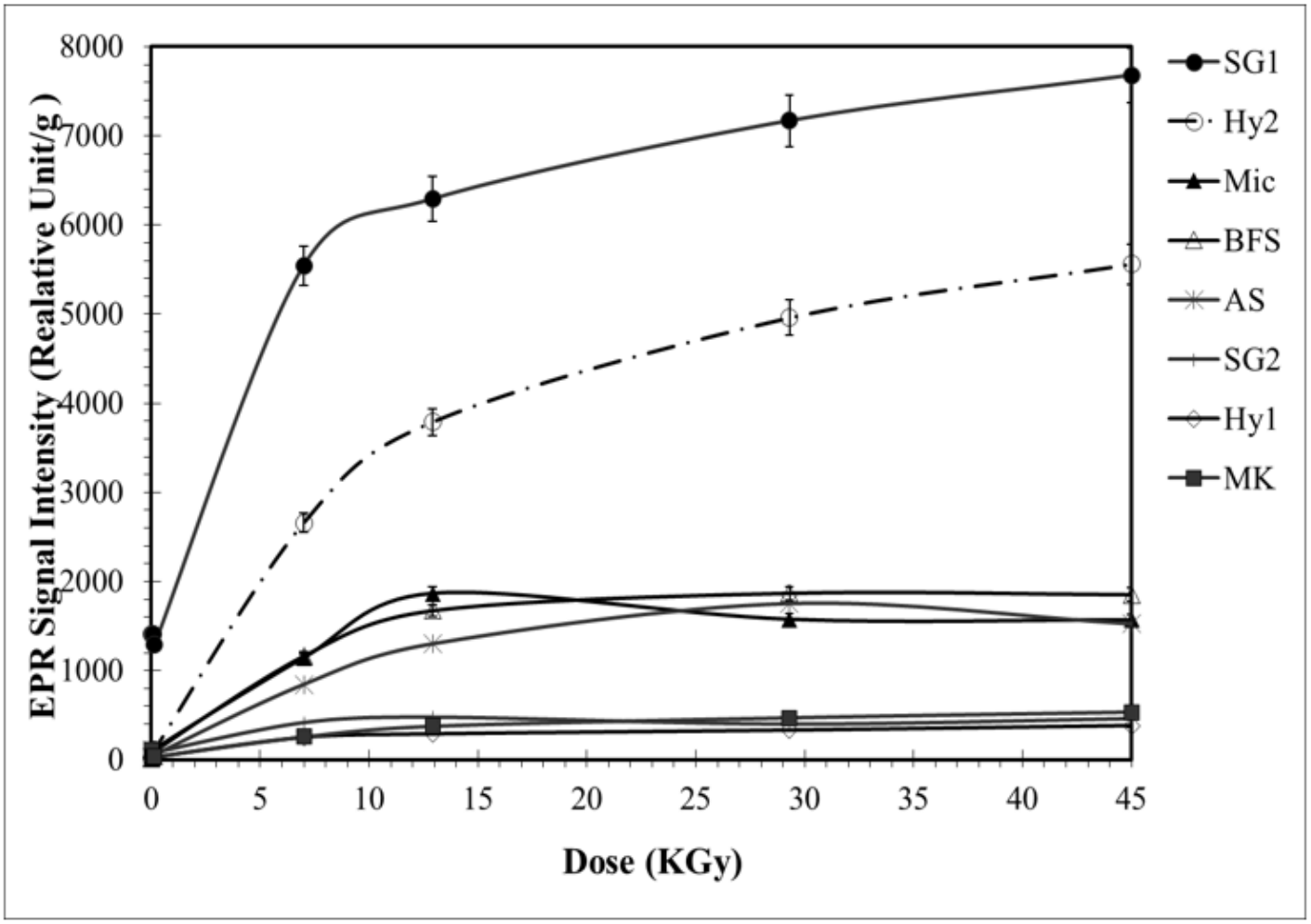

Figure 5

EPR signal intensity changes as a function of absorbed dose for synthetic HAp samples.